Digital holography microscopy in 3D biologic samples analysis

Journal of Physics: Conference Series **274** (2011) 012066 doi:10.1088/1742-6596/274/1/012066

Digital holography microscopy in 3D biologic samples analysis

J O Ricardo[1], M Muramatsu[2], F Palacios[1*], M Gesualdi[3], O Font[4], J L Valin[5], M Escobedo[6], S Herold[6], D F Palacios[7], G F Palacios[1] and A Sánchez[1]

[1] Department of Physics, University of Oriente, Cuba
[2] Department of General Physics, University of São Paulo - São Paulo, Brazil
[3] Engineering center, Models and Applied Social Science, UFABC - São Paulo, Brazil,
[4] Department of Bio-ingeniering, University of Oriente – Santiago de Cuba
[5] Mechanics Department, ISPJAE, Habana, Cuba
[6] Department of Computation, University of Oriente, Cuba.
[7] Department of Nuclear physics, University of Simón Bolíva, Venezuela

*Corresponding author's e-mail address: frpalaciosf@gmail.com

Abstract. In this work it is used a setup for Digital Holography Microscopy (MHD) for 3D biologic samples reconstruction. The phase contrast image reconstruction is done by using the Double propagation Method. The system was calibrated and tested by using a micrometric scale and pure phase object respectively. It was simulated the human red blood cell (erythrocyte) and beginning from the simulated hologram the digital 3D phase image for erythrocytes it was calculated. Also there was obtained experimental holograms of human erythrocytes and its corresponding 3D phase images, being evident the correspondence qualitative and quantitative between these characteristics in the simulated erythrocyte and in the experimentally calculated by DHM in both cases.

1. Introduction

The observation of a cells becomes very difficult firstly for its size and then for its transparency, it is for that reason that it is needed technical of optic microscopy that allow to obtain this information in a quick way and with great precision.

The Digital Holographic Microscopy (DHM), as a new digital microscopy technique has demonstrated phase measurements with interferometric resolutions, i.e. lateral micrometer range and sub-wavelength axial resolutions, of transparent biological specimens without the use of any contrast agent [1-3]. Compared to classical phase contrast and Nowarsky's differential interference contrast widely used in biology for the visualization of unstained transparent specimens, interferometric techniques present the significant advantage of yielding quantitative measurements of the phase shift produced by the specimen. The measured phase shift depends on both the refractive index and the thickness of the specimen, two quantities linked to the nature of the intracellular content and to the morphometry of the specimen, respectively. Because DHM allows for truly non-invasive examination of biological specimen, marker-free, no scanning required and online simultaneously [4,5], the interest of digital holography techniques for biomedical applications increases [6,7].

Computer modeling and simulation have become increasingly important aspects of modern research, and the DHM technique is no exception [8]. The two main reasons for computer based modeling and analysis are the verification of experimental data by reconciliation with theory and to

guide the process of experimental design. Although the verification aspects of the computer model are extremely useful, the simulations have taken on an even more important role in the essay of new reconstruction algorithms and methods of images analysis using the DHM.

Using the DHM a method for 3D image reconstruction of transparent microscopic objects, based on the capture of only one off-axis hologram and the reconstruction field at different locations along the propagation direction, have been proven [9,10]. Based on this possibility of the DHM, in this study it is demonstrated, through simulation techniques and experimental results, that DHM provides valuable information for the quantitative analysis of the 3D phase image reconstruction.

2. Experimental setup

Figure 1 shows the experimental setup used in this work, it correspond to a Digital Holographic Microscope designed for transmission imaging with transparent sample.

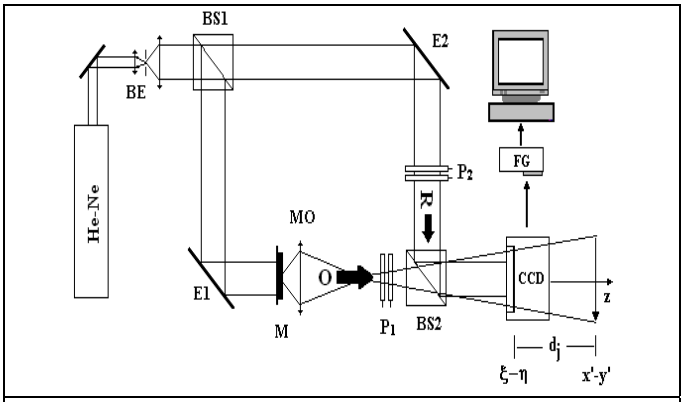

Figure 1. Experimental setup

A linearly polarized He-Ne laser (15 m W) is used as light source. The expanded beam from the laser is divided by the beam splitter (BS1) into reference and object arms. The microscope produces a magnified image of the object and the hologram plane is located between the microscope objective MO and the image plane (x'-y') at a distance d_j from the recording hologram plane (ξ-η). In digital holographic microscopy we can consider the object wave emerging from the magnified image and not from the object itself [11].

The specimen M is illuminated by a plane wave and a microscope objective ***MO*** that produces a wave front called object wave ***O***, collects the transmitted light. At the exit of the interferometer, the interference between the object wave ***O*** and the reference wave ***R*** creates the hologram intensity $I_H(\xi,\eta)$. A digital hologram is recorded by a CCD camera HDCE-10 with 4.65 µm of pixel size. The digital hologram $I_H(j,l)$ is an array of $M \times N$ = 768 x 768 8-bit-encoded numbers that results from the two-dimensional sampling of $I_H(j,l)$ by the CCD camera. For the image reconstruction is used the D*ouble* P*ropagation* M*ethod* (DPM) [23].

3. Reconstruction Method

Digital holography is based on the classic holographic principle, with the difference that the hologram recording is performed by a digital image sensor, e.g. a CCD or CMOS camera. The principle of recording holograms in holographic microscopy is shown in figure 2.

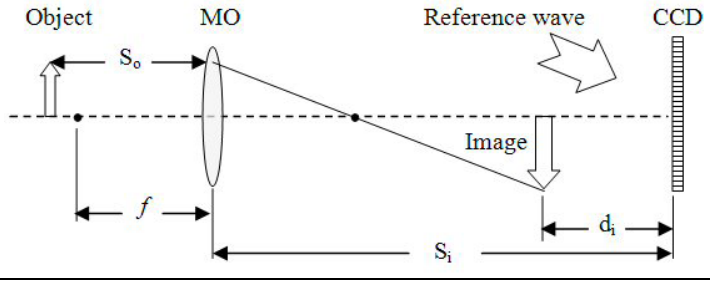

Figure 2. Hologram recording in DHM

The MO produce a magnified image of the object, and the hologram plane 0ξ (the CCD plane) is located between the MO and the image plane ($0x'$), at a distance d' from the image. This situation can be considered to be equivalent to a holographic configuration without magnification optics with an object wave emerging directly from the magnified image and not from the object itself. For this reason the term *image holography* is sometime used to designate this procedure. Classical microscopy can be achieved with this arrangement by translation of the object or the hologram plane such that the image is focused on the CCD.

A detailed description of the algorithm used for hologram reconstruction and the general reconstruction procedure has been previously described in [12]. In a few words, the reconstruction procedure consists in a simulation of the re-illumination of the hologram by a digital reference wave and a numerical correction of the wave front modifications induced by the objective and by the off-axis geometry. Mathematically, hologram reconstruction is carrying out calculating the diffracted field in the image plane by means of the Rayleigh-Sommerfeld diffraction formula. In this study the DPM method is used and briefly gives a simple description. In Digital Holographic Microscopy the field produced by the objective lens can be reconstructed along its propagation [13], figure 3a.

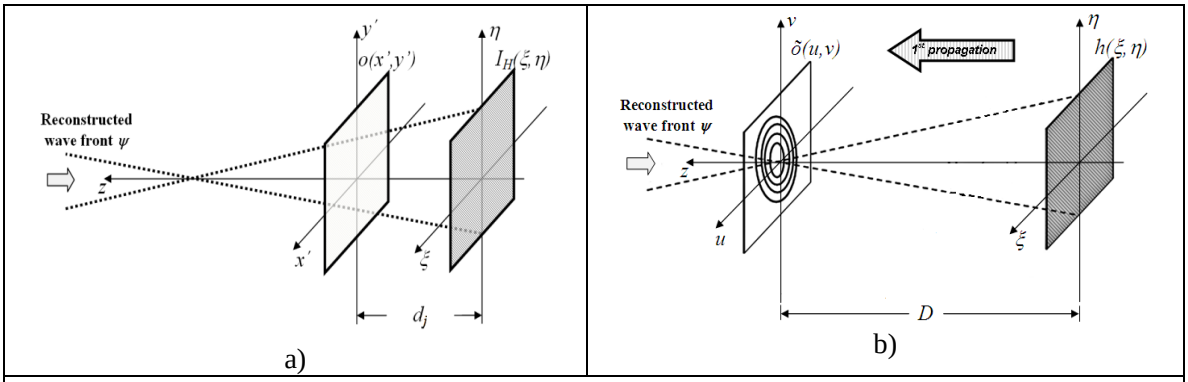

Figure 3. a) Image reconstruction in DHM, b) Reconstruction of the wave distribution $\tilde{o}(u,v)$ on the $(u\text{-}v)$ plane.

The reconstruction of the complex wave distribution $\tilde{o}(u,v)$ on the $(u\text{-}v)$ plane at reconstruction distance z = D, figure 3b, can be accomplish by means of the S*ingle* F*ourier* T*ransform* F*ormulation* (SFTF) [14]. The filtered complex wavefield in the same region defined by real image can be expressed by Eq. 1 by replacing the specimen hologram with a filtered hologram containing only spatial components of the real image [15],

$$\psi^{f}_{SFTF}(x',y',z=D)=A\exp\left[\frac{i\pi}{\lambda D}\left(x'^{2}+y'^{2}\right)\right]\Im\left\{I^{f}_{H}(\xi,\eta)\exp\left[\frac{i\pi}{\lambda D}\left(\xi^{2}+\eta^{2}\right)\right]\right\}_{[k_u,k_v]} \quad (1)$$

The complex field ψ^{f}_{SFTF} is equivalent to the complex field distribution $\tilde{o}(u,v)$ on the back focal plane of the objective lens. From the Abbe's theory of image formation [16], the field on the back focal plane is related with Fourier Transform of the objects.

Starting from the complex field described by Eq. (1), the complex wavefield $\psi(x',y',z=D,d')$ at an arbitrary d' can be obtained by propagation of the wavefield ψ^{f}_{SFTF} at the translational distance d' and the result is inverse Fourier transformed,

$$\psi(x',y',z=D,d') = \Im^{-1}\left\{\psi^{f}_{SFTF}(x',y',z=D)\exp\left(i\,d'\sqrt{k^2+k_u^2+k_v^2}\right)\right\} \tag{2}$$

where $\Im^{-1}$ denotes the inverse Fourier transform, $k=2\pi/\lambda$, k_u and k_v the spatial frequencies corresponding to u and v respectively.

From Eq. 2 we can obtain the amplitude image $I(x',y',d'=d_j)$ by calculating the intensity,

$$I(x',y',d'=d_j) = \mathrm{Re}\left[\psi(x',y',z=D,d'=d_j)\right]^2 + \mathrm{Im}\left[\psi(x',y',z=D,d'=d_j)\right]^2 \tag{3}$$

and the phase image $\phi(x',y',d'=d_j)$ by calculating the argument,

$$\phi(x',y',d'=d_j) = arc\tan\left\{\frac{\mathrm{Im}\left[\psi(x',y',z=D,d'=d_j)\right]}{\mathrm{Re}\left[\psi(x',y',z=D,d'=d_j)\right]}\right\} \tag{4}$$

4. Lateral and Axial testing

For lateral testing and calibration the capture of one hologram was performed in the working conditions. The intensity and phase image reconstruction was done, figure 4, in this case for the micrometric scale *Mitutoyo®* with 100 lines per mm as object proves.

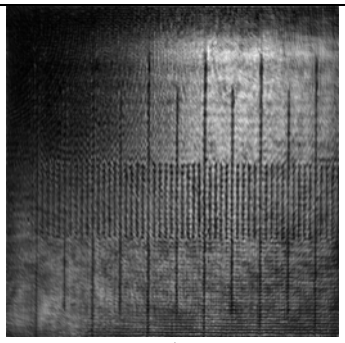

a)

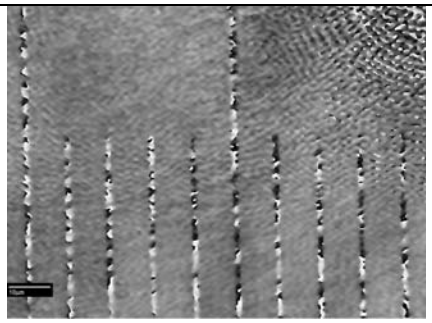

b)

Figure 4. Reconstructed Images for system calibration. a) Intensity with the objective of 12.5x/0.35 and b) Phase with the objective 50x/0.95.

For axial testing a pure phase object was used. It consists of a portion of a character engraved on a glass substrate. In figures 5a it is shows the hologram and in figure 5b and 5c are show the phase image and the pseudo 3D phase image respectively.

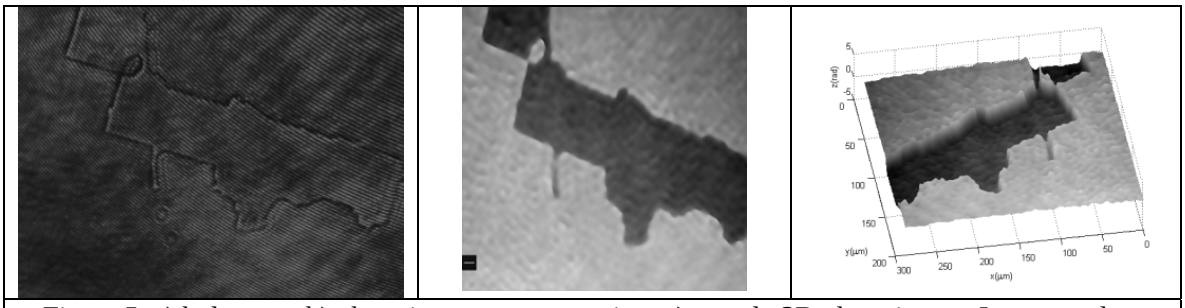

Figure 5. a) hologram, b) phase image reconstruction, c) pseudo 3D phase image. It was used an objective of 12.6x/.35

A quantitative and qualitative evaluation in lateral and axial image shows the capacities of the system for the representation with good quality a 3D perspective of the studied object.

5. Simulation technique

The simulated object is a normal human red blood cell. Taking as the object model the bibliography image [17], figure 6a, we consider homogeneous refractive index *(n ≈ 1.4)*, diameter $d_r = 7.7\ \mu m$, height variation from $h \approx 2.5\ \mu m$ to $h_e \approx 0.6\ \mu m$ in the central part and inner in air *(n = 1)*. Considering the form of the red blood cell transversal section, it can be represented by the Cassini oval, figure 6b.

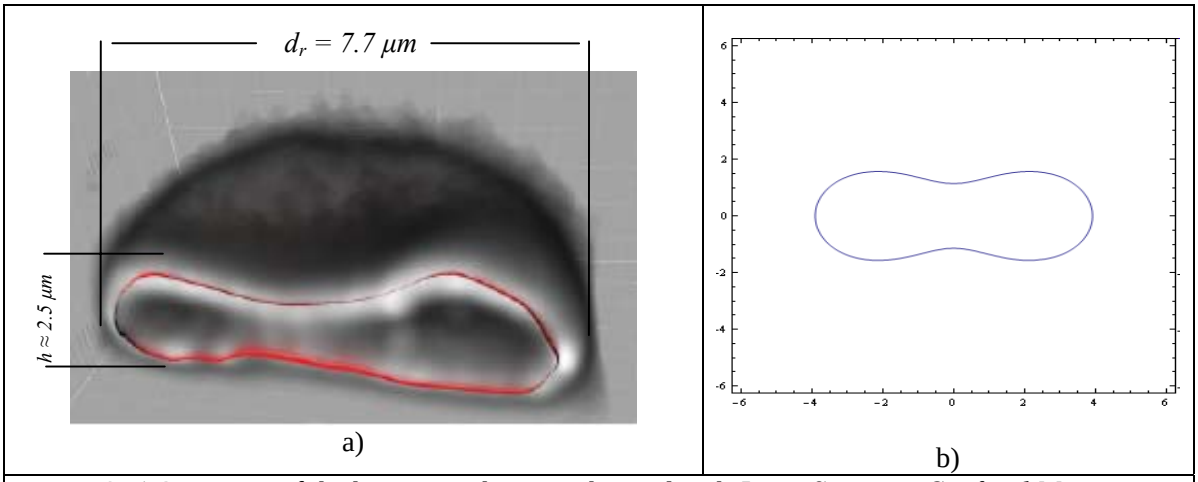

a) b)

Figure 6. a) 3D Image of the human erythrocyte obtained with *Laser Scanning Confocal Microscopy*. b) Bidimensional view of the Cassini oval.

Starting from the expression of the Cassini oval:

$$(x^2 + y^2)^2 - c^2(x^2 - y^2) = a^4 - c^4 \tag{5}$$

the volumetric expression of the object is obtained from the equation,

$$V = (x^2 + y^2)^2 - c^2(x^2 - z^2) - c^2(y^2 - z^2) - a^4 + c^4 \tag{6}$$

Figure 7a show the representation of the Eq. (6) and the transversal section in the *y-z* plane where can be observed the Cassini oval in figure 7b.

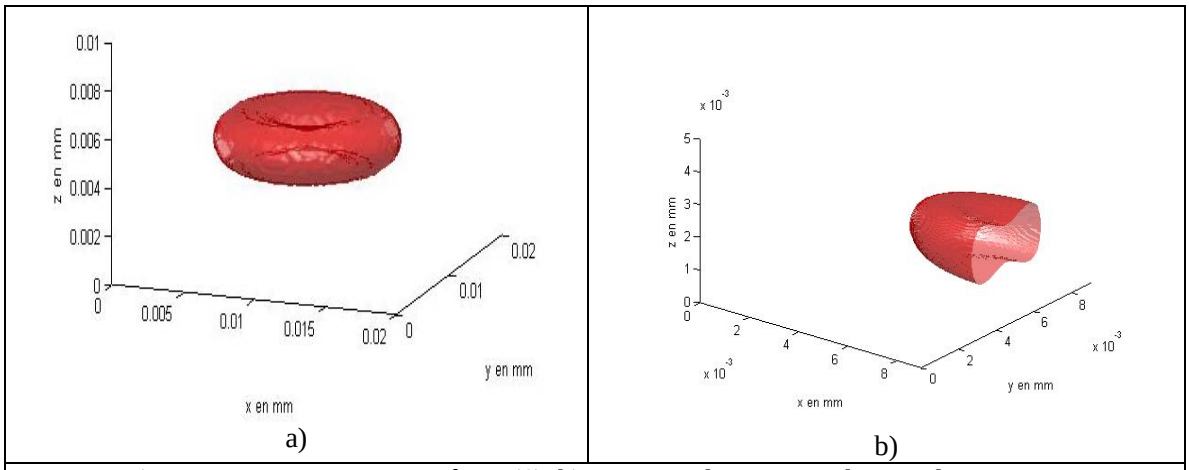

Figure 7. a) Numeric representation of Eq. (6), b) transversal section in the *y*-z plane.

For this simulation it was used the MatLab© system for the 0.010x0.011x0.011 mm^3 volume calculation with the parameters $a = 3.01$, $c = 3.00$ for Eq. (6). With the variation of these parameters can be obtained various forms of the Cassini oval and thus more accurately represent a real erythrocyte. The simulated hologram is according with the DHM principles, it was simulated the image produced by a lens taking into account as object the volume 7a. Superposing this image with a plane reference beam it is generating the digital simulated hologram, shows in figure 8a. Using the DPM method it was reconstructed phase image, figure 8b. Figure 8c shows the transversal section profile of the phase image represented in 8b.

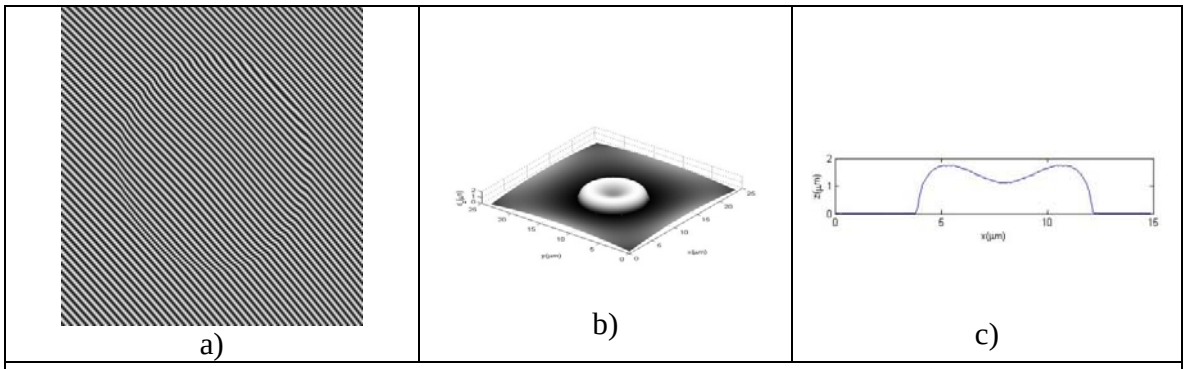

Figure 8. a) Simulated Digital Hologram, b) Reconstructed phase image, c) profile of the transversal section of phase image.

6. Experimental Results

From one sample of human blood cell marker-free and the experimental setup showed in figure 1, were done measurements for obtaining the reconstructed phase image.

The Microscopic system calibration was done using reconstructed phase image using objective of 50x/0.85. The corresponding hologram is showed in figure 9a and the figure 9b shows a section of a hologram of human blood sample, where can be seen the holograms characteristics interferences micro fringes of the image hologram.

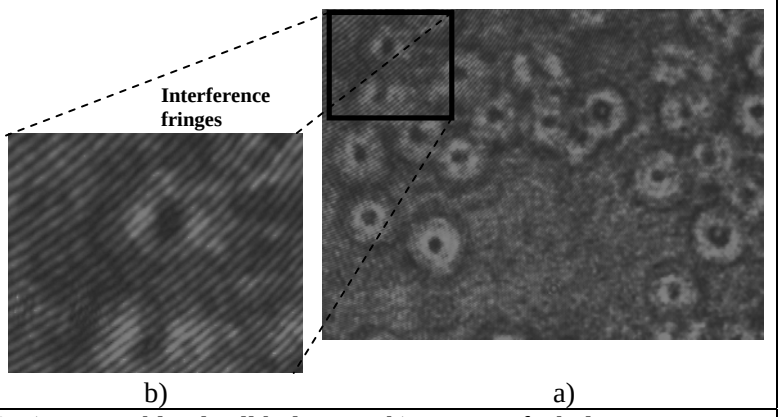

Figura 9. a) Human blood cell hologram. b) section of a hologram

The figures 10a and 10b shows the phase image in perspective 2D and 3D respectively, in c) the transversal section from de red cell in the phase image of 10a. The cell thickness *z* it was calculated considering the refractive index *n = 1.4.*

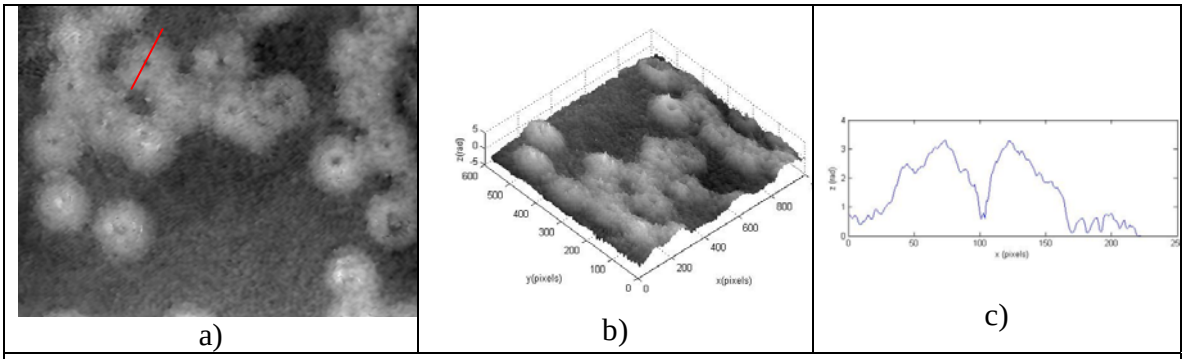

Figure 10. a) Reconstructed phase image, b) pseudo 3D image and c) transversal section in red on the phase image 9a.

From figure 10c the thickness *z* agrees with the reported in specialized literature [17].

7. Conclusions

In these work it was demonstrated the potentiality of DHM for microscopic objects image visualization like cells of biological interest, being simple its application and after system be adjusted and calibrated it don't require big experimental abilities. The technique of DHM it was implemented by simulated and experimental way, both results qualitatively are similar taking into consideration that the simulated system don't consider the erythrocyte resting upper the glass port object like in the experimental system. The method might be applied for others micro samples.

8. Acknowledgements

This work was supported by the Brazilian agency FAPESP; Process FAPESP No. 2009/50438-7, PV-Prof. Jorge O. Ricardo Perez in July 2009-january 2010.

9. References

[1] Marquet P, Rappaz B, Magistretti P, Cuche E, Emery Y, Colomb T, and Depeursinge C 2005 Digital holographic microscopy: a non invasive contrast imaging technique allowing quantitative visualization of living cells with subwavelength axial accuracy *Opt. Lett*. **30**:468

[2] Carl D, Kemper B, Wernicke G, and Von Bally G 2004 Parameter-optimized digital holographic microscope for high-resolution living-cell analysis *Appl. Opt***. 43** 6536

[3] Ikeda T, Popescu G, Dasari R, and Feld M 2005 Hilbert phase microscopy for investigating fast dynamics in transparent systems *Opt. Lett*. **30** 1165

[4] Kemper B, Carl D, Höink A, Von Bally G, Bredebusch I, Schnekenburger J 2006 Modular digital holographic microscopy system for marker-free quantitative phase contrast imaging of living cells *Proc. SPIE 6191*

[5] Von Bally G, Kemper B 2006 New ways for marker free life cell and tumor analysis ***(****MIKROSO, in: J. Popp, M. Strehle Eds.): Bioph. Vis. for a better Health Care,* Wiley, S. 301

[6] Tishko T, Titar V and Tishko D 2005 Holographic methods of three dimensional visualization of microscopic phase objects *J. Opt. Technol.* **72(2)** 203

[7] Massatsch P, Charrière F, Cuche E, Marquet P and Depeursinge C 2005 Time domain optical coherence tomography with digital holographic microscopy *Appl. Opt.* **44** 1806

[8] Grilli S, Ferraro P, De Nicola S, Finizio A, Pierattini G, Meucci R 2001 Whole optical wavefields reconstruction by Digital Holography *Opt. Exp.* **9** 294

[9] Palacios F, Ricardo J, Palacios D, Gonçalves E, Valin J, De Souza R 2005 3D image reconstruction of transparent microscopic objects using digital holography *Opt. Commun.* **248** 41

[10] Palacios F, Palacios D F, Goncalves E, Palacios G, Sajo-Bohus L, Ricardo J, Valin J 2010 3D nuclear track analysis by digital holographic microscopy *Radiat. Meas.* doi: 10.1016/j.radmeas.2010.08.011

[11] VanLigten R F and Osterberg H 1966 Holographic microscopy *Nat.* **211** 282

[12] Cuche E, Marquet P, and Depeursinge C 1999 Simultaneous amplitude-contrast and quantitative phase contrast microscopy by numerical reconstruction of Fresnel off-axis holograms *Appl. Opt*. **38** 6994

[13] Palacios F, Palacios D, Palacios G, Gonçalves E, Valin J, Sajo-Bohus L, Ricardo J 2008 Methods of Fourier optics in digital holographic microscopy, *Opt. Commun.* **281** 550

[14] Kreis T and Jüpner W 1997 Principles of digital holography *Akademie Verlag (Series in Opt. Met.)* **3** 353

[15] Cuche E, Marquet P, and Depeursinge C 2000 Spatial filtering for zero-order and twin-image elimination in digital off-axis holography *Appl. Opt*. **39** 4070

[16] Lipson S G, Lipson H 1981 *Optical Physics* (Sec. Ed., Cambridge Univ. Press).

[17] Rappaz B, Barbul A, Emery Y, Korenstein R, Depeursinge C, Magistretti P J, Marquet P 2008 Comparative study of human erythrocytes by digital holographic microscopy, confocal microscopy and impedance volume analyzer *J. Inter. Soc. for Adv. of Cyt. Part A* ***73A*** 10 895